Catalytic Pyrolysis of Corn Stalk for the Production of Aromatics: The Effects of Wet Torrefaction and Zn/Ni-HZSM-5 on Pyrolysis Behavior

Jiaqi Zhang, Qi Zhang, Zhijing Sun, Fang Wang, Lu Di, Deli Zhang,* and Weiming Yi *

The pyrolysis of corn stalk (CS) was carried out to investigate the effect of wet torrefaction (WT) pre-treatment and Zn/Ni-HZSM-5 on the production of bio-oil characteristics. The synergy between WT and the loaded metal catalyst was also analyzed. The oxygen content of the CS was reduced from 50.5% to 40.8% with WT, and hemicellulose was almost removed. WT pretreatment also significantly reduced the oxygenated compounds of bio-oil and increased the selectivity of phenols, aromatics, and anhydro-sugars. The addition of catalyst improved the deoxygenation, oligomerization, and aromatization during pyrolysis. The loading of Zn and Ni could optimize the pyrolysis reaction path and increased the relative content of monocyclic aromatics (MAHs) from 3.58% to 9.67% and 6.44% during the pyrolysis of CS-WT, respectively, and bimetallic catalyst further enhanced the relative content of MAHs to 11.1%. The relative content of aromatics below C9 was higher than other groups (14.8%). Thus, the WT pretreatment of raw materials and synergistic effect of catalysts can jointly optimize the biomass pyrolysis reaction.

DOI: 10.15376/biores.18.3.4897-4915

Keywords: Wet torrefaction; Corn stalks; Catalytic pyrolysis; Bimetallic catalyst; Aromatics selectivity

Contact information: School of Agricultural Engineering and Food Science, Shandong Research Center of Engineering & Technology for Clean Energy, Shandong University of Technology, Zibo 255000 China;
** Corresponding authors: zhangdeli@sdut.edu.cn; yiweiming@sdut.edu.cn*

INTRODUCTION

With the rapid growth of the global economy, the demand for energy fuels is increasing. However, fossil fuels are facing the double pressure of energy shortage and environmental pollution. Lignocellulosic wastes have received attention for their abundant reserves, renewability, carbon neutrality, and suitability for conversion into liquid fuels and chemical feedstock (Wang *et al.* 2017). Because of the short reaction time and higher conversion rates, fast pyrolysis is a research hotspot. However, biomass has the problem of complex structure, low volumetric energy density, and high oxygen content. These negative properties have resulted in quality problems of bio-oil such as poor product selectivity, high acidity, and complicated reaction processes (Lu *et al.* 2009).

Pretreatment of biomass feedstocks is important to optimize biomass composition. In wet torrefaction (WT), also known as hydrothermal pretreatment, biomass is heated in a hot compressed water environment to optimize the structure of its components (Bach *et al.* 2015). In WT, the hemicellulose in the biomass is turned almost completely into water-soluble compounds, and the sealing property of the lignin is broken, while most cellulose and lignin structures are preserved (Zhang *et al.* 2018). WT pretreatment can reduce the proportion of inorganic matter in the raw material and transfer it to the liquid phase product,

thereby reducing the ash content in the solid phase product (Danso-Boateng and Achaw 2022). WT can greatly reduce the oxygen content and acidity of bio-oil, and increase the fuel value of bio-oil (Xu *et al.* 2022). Ge *et al.* (2020) showed that due to pyrolysis of eucalyptus produces bio-oil, the yields of acids and ketones decreased significantly, and the yields of aromatics and L-glucose increased with the WT pre-treatment of the biomass. Xu *et al.* (2018) studied the composition distribution of the pyrolysis products of *Camellia oleifera* shell after WT, finding that the acid yield of the bio-oil decreased from 34.5% to 13.2% and the phenols were enriched (from 27.2% to 60.0%). Therefore, the pretreatment of WT could optimize the quality of bio-oil for biomass, by reducing the acid yield of bio-oil and generating aromatics and phenols.

Another way to improve the quality of pyrolyzed bio-oils is to use catalysts to target the components of bio-oils. Zeolite catalysts represented by HZSM-5 have high specific surface area, uniform pore distribution, good shape selectivity, and a large number of strong acid sites, which have been widely used for biomass pyrolysis. Metal loading on HZSM-5 could optimizes the performance of the catalyst while reducing the coking of the reaction, and different loaded metals have different changes in the pyrolysis reaction pathway (Liu *et al.* 2021). Among them, Zn and Ni have higher selectivity for aromatics in bio-oil. Liang *et al.* (2017) used Ni, Co, and Zn modified ZSM-5 to catalyze the pyrolysis of dry straw and found that Ni and Zn enhanced the yield of guaiacol (from 6.25% to10.91%) and hydrocarbons (from 6.51% to 6.68%) in bio-oil, respectively. Dai *et al.* (2019) used NaOH-treated Ni-HZSM-5 catalyst to pyrolyze the torrefy corncob. The result was that Ni reduced the surface area, micropore volume, and acidity of the catalyst, and it enhanced the aromatic yield. Huang *et al.* (2020) studied the effect of Ga/Zn-HZSM-5 on the pyrolysis products of Masson pine and found that Ga and Zn had a significant synergistic effect on the selectivity improvement of benzene series products. Xu *et al.* (2019) studied the effect of Zn/Fe modified catalyst on the catalytic pyrolysis of *Eucalyptus* to aromatics; under the catalysis of 1% Zn-4 % Fe/HZSM-5, the yields of benzene, toluene, xylene, and naphthalene were 98.3%, 80.9%, 26.4%, and 49.0% higher than those catalyzed by HZSM-5, respectively. A synergistic effect was found between different metals, which can effectively improve the selectivity of single-ring aromatics and reduce the generation of coke compared with the single-metal modified catalysts.

WT can optimize biomass feedstock composition and have a positive effect on the selectivity of aromatics in the catalytic pyrolysis of biomass; metal-loaded catalysts can improve the directional selectivity of bio-oil product components (Liang *et al.* 2017; Xu *et al.* 2018; Liu *et al.* 2021). However, the synergistic effect of WT and loaded HZSM-5 in the pyrolysis process requires clarification. The selectivity of loaded metals to different components of biomass before and after WT is also unclear.

In this study, modified HZSM-5 (Zn and/or Ni loaded) were prepared and characterized. They were used to pyrolyze corn stalk (CS) and wet-torrefied corn stalk (CS-WT) to produce aromatics. The uncatalyzed pyrolysis and HZSM-5 catalytic pyrolysis were used as the control group. The objectives of this study were to understand the characteristics of CS and CS-WT, the effect of WT on the reaction path of catalytic pyrolysis, and the role of HZSM-5 loaded with Zn and Ni in the pyrolysis reaction of CS-WT. Furthermore, the synergistic effects of bimetallic catalysts versus monometallic catalysts were explored. This study was aimed to promote the targeted optimization of the reaction of biomass pyrolysis to improve the selectivity of target products.

EXPERIMENTAL

Materials

Corn stalks were collected from Zibo, Shandong Province, China. The feedstock was pulverized to 40- to 60-mesh and dried at 105 ℃. The HZSM-5 catalyst (SiO_2/Al_2O_3=38) was purchased from The Catalyst Plant of Nankai University, and was calcined in a muffle furnace at 550 ℃ for 10 h before use. $Ni(NO_3)_2{\cdot}6H_2O$ and $Zn(NO_3)_2{\cdot}6H_2O$ were purchased from YuanDong Chemical Reagent Company.

Catalyst Synthesis

The Ni/Zn metal modified HZSM-5 was prepared by the wet impregnation method (Tursunov *et al.* 2019). First, 10 g of HZSM-5 and $Ni(NO_3)_2{\cdot}6H_2O$ / $Zn(NO_3)_2{\cdot}6H_2O$ with calculated mass were dissolved in 50 mL of deionized water, and stirred for 10 h in a water bath at 60 ℃. The stirring speed was 100 r/min. The mixture was calcined oxygen-free at 600 ℃ for 10 h in a muffle furnace to obtain Ni/Zn-loaded HZSM-5. The loadings of the modified metals were 8% Zn, 8% Ni, and 4% Zn+4% Ni, which were denoted as Zn-HZSM-5, Ni-HZSM-5, and Zn/Ni-HZSM-5, respectively.

Preparation of Samples

WT was carried out in a stainless-steel autoclave. The mixture (corn stalk: deionized water = 1:10) was put into the autoclave, the autoclave was sealed, and then normal pressure nitrogen was passed through as the reaction atmosphere. The autoclave was heated from ambient temperature to 220 ℃ and kept for 10 min, during which the stirring speed was 100 r/min. After the completion of the reaction, cooling water was passed into the autoclave to cool it, and the reactants were collected and filtered. The collected solid phase was dried in an oven at 105 ℃ overnight, then weighed. The yield was calculated; the liquid phase was stored at -4℃. The corn stalk before and after WT was denoted as CS and CS-WT, respectively.

Catalyst Characterization

The crystal structure of the catalyst was evaluated using a polycrystalline X-ray diffractometer (Bruker AXS D8 Advance, Karlsruhe, Germany). Cu-Kα radiation was generated at 40 kV and 50 mA, with 2θ ranging between 3°and 50° at 0.02°/min.

An ASAP 2020 analyzer (Micromeritics, Norcross, GA) was used to characterize the specific surface area, pore volume, and pore size characteristics of the catalyst. The catalyst was first degassed at a temperature of 300 ℃ for 3 h, and then it was subjected to a nitrogen adsorption test at a temperature of -196 ℃. The specific surface area was calculated by the Barrett-Emmett Teller (BET) method, and the pore volume and average pore diameter were calculated by the Barrett-Joyner-Halenda (BJH) method.

An AutoChem II 2920 (Micromeritics, Norcross, GA) apparatus was used for the NH_3-TPD analysis to measure the acid properties of the catalyst. A sample of 50 mg was preheated at 550 ℃ with a He flow (30 mL/min) for 30 min to remove the adsorbed moisture from the sample. The sample was cooled to 100 ℃ and allowed to adsorb NH_3 at 100 ℃ for approximately 60 min until saturation. Finally, after obtaining a stable baseline, under the purge of He gas, the sample was heated to 700 ℃ at a rate of 10 ℃/min for desorption. The desorbed NH_3 was monitored using a thermal conductive detector (TCD) during the TPD process.

Biomass Analysis

According to Van Soest, a Semi-automatic cellulose Analyzer (A200i, ANKOM, USA) was used for the determination of cellulose, hemicellulose, and lignin in feedstock. The element analysis was performed on the Vario EL cube type element analyzer (Elementar, Langenselbold, Germany). The test temperature was 1000 ℃, while oxygen and a high temperature oxidizer were used as additives; each sample was tested twice.

The thermogravimetric analysis of CS and CS-WT was analyzed via simultaneous thermal analyzer (STA449F5, NETZSCH, Germany). The test temperature was 45 to 900 ℃, the carrier gas was He, and each sample was tested twice.

The composition of the bio-oil was analyzed via gas chromatography-mass spectrometry (8890-5973, Agilent, Santa Clara, CA). A DB-1701 capillary column (60 m × 0.25 mm × 0.25 μm) was used to separate the bio-oil components. The temperature of the injector and the AUX were set to 280 and 230 ℃, respectively. The GC oven was heated from 40 to 240 ℃ at a rate of 5 ℃/min and then maintained at that temperature for 5 min. The carrier gas was high purity helium (99.999%), and the constant flow rate was 1 mL/min. The mass spectrometry analysis was carried out in EI mode. The ionization energy was 70 eV, and the scanning range was (*m*/*z*) 12 to 750 amu. Based on the NIST 17 library, the detailed chemical information corresponding to the chromatographic peak was determined.

In each experiment, the chromatographic peak area of each product was recorded, and then the relative content (peak area %) was calculated by dividing the peak area (target product) by the total peak area (all tested products). The peak area % was used to represent the selectivity of the product.

Pyrolysis Process of Biomass

A pyrolysis device is primarily composed of a carrier gas device, horizontal tube horizontal reactor, temperature controller, and cooling system. The pyrolysis reactor used in this work was a quartz tube (700mm*Φ60mm*3mm). The cooling system consisted of two cold traps and a cooling box. The cooling medium was mixture of ethylene glycol and water (volume ratio 1:2) at a temperature of -10 ℃. The pyrolysis temperature was 550 ℃, and the ratio of raw material to catalyst was 1:3. Nitrogen was used as the pyrolysis carrier gas, and the flow rate was 800 ml/min.

Four different catalysts (HZSM-5, Zn-HZSM-5, Ni-HZSM-5, and Zn/Ni-HZSM-5) were mixed with CS and CS-WT for pyrolysis, respectively, while the feedstocks were used for pyrolysis alone as a control. Before each pyrolysis experiment, the tubular reactor was purged with high-purity nitrogen for a period of time. Once the reactor temperature reached the set value (550 ℃), the quartz boat was immediately pushed into the pyrolysis zone. The process lasted for 10 min. Finally, the reactor was cooled to room temperature in a nitrogen atmosphere.

The quartz boat and cold trap before and after the reaction were weighed, and the yields of biochar and bio-oil were calculated, and the yields of non-condensate gas were calculated via mass balance calculation. Each experiment was repeated twice to ensure the reproducibility of the experiment.

RESULTS AND DISCUSSION

Properties of Modified Catalysts

XRD analysis

The XRD patterns of the HZSM-5 catalyst and modified HZSM-5 (Zn-HZSM-5, Ni-HZSM-5, and Zn/Ni-HZSM-5) are shown in Fig. 1. The HZSM-5 catalyst had five typical characteristic diffraction peaks at 2θ=7.92°, 8.81°, 23.06°, 23.88°, 24.34°, which were in line with the topology and standard characteristics of molecular sieve catalysts (Balasundram *et al.* 2017). The diffraction peak positions of the metal-loaded catalyst did not change, indicating that the lattice structure of the catalyst was maintained after the metal loaded. No characteristic peak of ZnO crystal phase were found at 2θ=34.5°and 36.3°. Similarly, there were no characteristic peaks of NiO crystal phase at 2θ=37.2°and 43.2° (JCPDS 65-2901). These indicated that both Zn and Ni were dispersed in the surface or in the pores of the molecular sieve in the form of amorphous or highly dispersed small particle morphology (Cheng *et al.* 2017). The peak intensity of the catalyst decreased as the metal was loaded. The reason is that the precursor of loaded metals can slightly damage the molecular sieve framework.

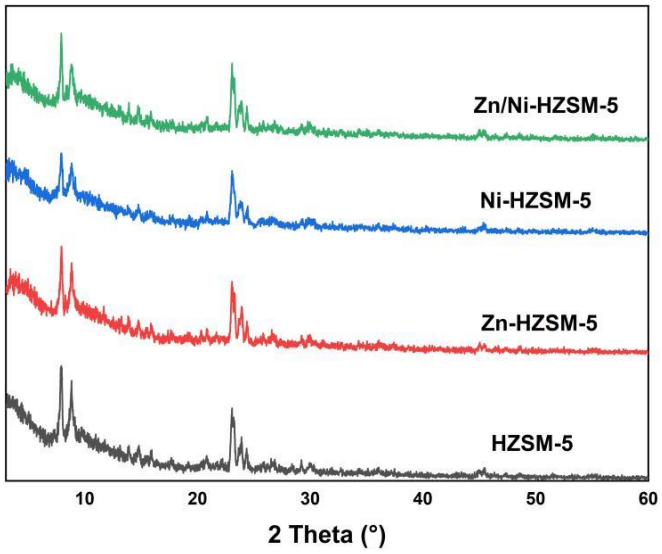

Fig. 1. X-ray diffraction spectra of HZSM-5 and modified HZSM-5

BET analysis

The structural properties of the catalysts were investigated by N_2 physisorption and desorption isotherm curves, as shown in Fig. 2. Table 1 shows the surface area, pore volume, and pore size of the catalysts. The adsorption-desorption curves of all catalysts were of type IV, with obvious hysteresis loops, and the shape of the curves did not change after the metal was loaded, indicating that all of the molecular sieve catalysts had graded micropores and mesopores (Bjørgen *et al.* 2008). The hysteresis loops of all catalysts were reduced after metal loading. The order of hysteresis loop size was HZSM-5>Zn/Ni-HZSM-5>Ni-HZSM-5>Zn-HZSM-5, which indicated that the metal occupies part of the pore channels, resulting in the reduction of the pore volume (Zheng *et al.* 2017). Zn is easily deposited in the pores of HZSM-5, while Ni is more loaded on the surface of the catalyst (Foster *et al.* 2012; Gao *et al.* 2021).

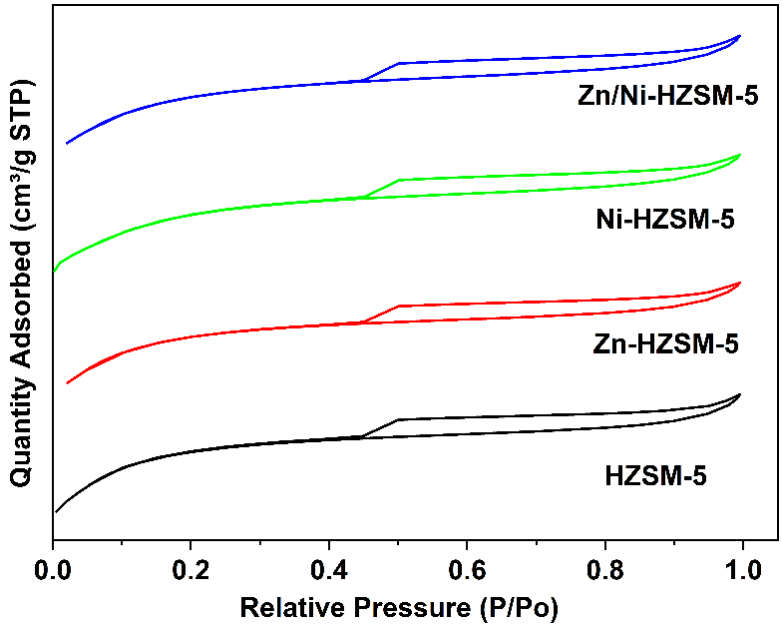

Fig. 2. Porosity characteristics of HZSM-5 and modified HZSM-5

Table 1. Surface and Pore Properties of the Catalysts

catalysts	Area (m^2/g)		Volume (cm^3/g)		Average pore diameter (nm)
	Micropore	External Surface	Micropore	Mesopore	
HZSM-5	240.47	109.81	0.1186	0.0758	2.22
Zn-HZSM-5	234.15	109.38	0.1153	0.0741	2.21
Ni-HZSM-5	219.75	121.51	0.1084	0.0823	2.23
Zn/Ni-HZSM-5	229.53	114.04	0.1140	0.0797	2.25

Compared with HZSM-5, the pore volume and specific surface area of the metal-loaded catalyst were decreased, and the average pore size was increased. After loading, part of the metal oxides were deposited in the pores of the catalyst to block the internal channels of the molecular sieve, whereas others were attached to the surface of the catalyst (Cheng *et al.* 2018). Zn and Ni were evidently different in the load position: Compared with the uniform loading of Zn on micropores and mesopores, the micropore area and micropore volume of the Ni-modified catalyst decreased greatly, while the external surface area and mesopore volume increased significantly. This was consistent with the changing trend of the hysteresis loops. Ni tends to agglomerate and block micropores, and forms new mesoporous structures at high loading concentrations (Gao *et al.* 2021). Compared with Zn-HZSM-5 and Ni-HZSM-5, the agglomeration effect of Zn/Ni-HZSM-5 was weakened due to the decrease of the respective loadings of Zn and Ni, and the distribution of loading sites became more balanced. Zn/Ni-HZSM-5 reduced the effect of loading on micropores while increasing the external surface area and mesopore volume, which might play an important role in improving the yield of aromatics in catalytic pyrolysis (Qiao *et al.* 2019). In conclusion, compared with Zn or Ni, the Zn+Ni composite modification could optimize the pore size distribution of HZSM-5 better and make it have better surface properties.

NH_3-TPD analysis

NH_3-TPD was used to characterize the strength of acid sites in catalysts. As shown in Fig. 3, HZSM-5 had two desorption peaks at 130 to 250 ℃ and 280 to 430 ℃, corresponding to the weak acid and strong acid sites of the catalyst, respectively. After the metal supporting, the areas of the strong acid peak and the weak acid peak of the catalyst decreased, and the positions of the peaks moved to the low temperature direction. Numerous studies had concluded that when the number of acid sites was sufficient, the acid protons on the Brønsted acid were substituted by Zn^{2+} and Ni^{2+} to become Lewis acids, resulting in a decrease in the surface acidity of HZSM-5 (Zhao *et al.* 2015), which is consistent with the conclusion of Fig. 3. Generally, Brønsted acid and Lewis acid can facilitate the formation of carbocation and hydrogen transfer, respectively. Brønsted acid can promote alkene cyclization, decarbonylation, and decarboxylation reactions, but also improve coke yield. In addition, Lewis acid can promote the formation of olefins and MAHs, inhibit polycyclic aromatics (PAHs), and also promote the dehydration reaction (Rostamizadeh *et al.* 2018).

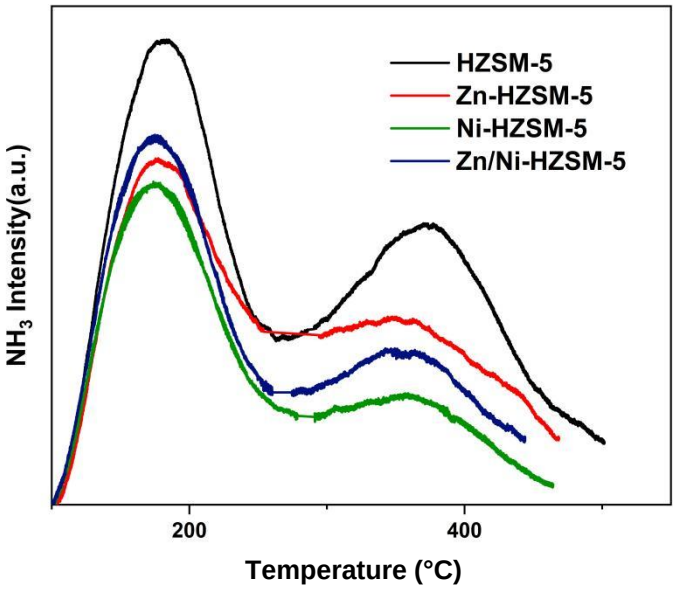

Fig. 3. Ammonia desorption curve of HZSM-5 and modified HZSM-5

Figure 3 shows that the weak acid peaks of Zn-HZSM-5, Ni-HZSM-5, and Zn/Ni-HZSM-5 were close, but the variation range of the strong acid peaks were very different, which indicated that the metal loading mainly affected the strong acid. The strong acid peak, weak acid peak, and the peak area of Ni-HZSM-5 were the lowest, indicating that the blockage of catalyst pores by Ni was more serious than that of Zn (Vitale *et al.* 2013). The strong acid peak of Zn-HZSM-5 had the smallest decrease and was adjacent to the weak acid peak, showing that Zn was uniformly loaded on the acidic site of HZSM-5, converting Brønsted acid to Lewis acid (Cheng *et al.* 2017). The weak acid peak of Zn/Ni-HZSM-5 was higher than that of Zn-HZSM-5 and Ni-HZSM-5, and the strong acid peak was between Zn-HZSM-5 and Ni-HZSM-5. It confirms the effect of Ni on the strong acid sites, while indicating that Zn^{2+} and Ni^{2+} would convert it into a weak acid. The acidity reduction of Zn/Ni-HZSM-5 was suitable when the oxygen content of biomass decreased, and low acidity catalysts could inhibit the formation of PAHs (Qiao *et al.* 2019).

Effects of WT on the Feedstock

Physicochemical properties

The elemental analysis and lignocellulosic analysis of CS and CS-WT are shown in Table 2. After WT, the hemicellulose content decreased from 29.2% to 3.98%, while the cellulose and lignin increased from 36.5% and 3.07% to 57.8% and 10.1%, respectively. These findings indicated that hemicellulose was almost completely decomposed during WT, while the structure of cellulose and lignin remained stable, which is in accorded with other research findings (Wang *et al.* 2018). The study of Danso-Boateng showed that hemicellulose was almost decomposed at 220 ℃, while cellulose was only partially decomposed. Lignin has a stable phenolic structure, and the decomposition temperature is close to 250 ℃ (Danso-Boateng *et al.* 2022). Zheng *et al.* (2015) found that hemicellulose is composed of short-chain heteropolysaccharides, exhibits an amorphous and branched structure, has a low degree of polymerization, and is easily decomposed under mild WT conditions.

Table 2. Elemental Analysis and Lignocellulosic Analysis of CS and CS-WT

Materials	Element (%)				Component (%)			HHV (MJ/Kg)
	C	H	O	N	Hemicellulose	Cellulose	Lignin	
CS	42.92	5.62	50.47	0.77	29.19	36.50	3.07	17.101
CS-WT	51.94	5.88	40.83	0.88	3.98	57.77	10.10	20.765

After WT, the carbon content of CS-WT increased from 42.9% to 51.9%, the oxygen content decreased from 50.5% to 40.8%, and the hydrogen content did not change significantly. This was because the oxygen element was removed by decarboxylation and dehydroxylation during the WT process (Li *et al.* 2020). The branched chains of hemicellulose contain a large amount of uronic acid and acetyl groups, from which it is easy to generate oxygen-containing compounds, which is not conducive to the directional regulation of products (Wang *et al.* 2017). In this experiment, WT removed most of the hemicellulose, weakening the compositional complexity of the pyrolysis reaction feedstock, which could reduce the acidity and oxygen content of the bio-oil. The reduction of acetyl and oxygen elements also means that the need for the decarboxylation and deoxidation capacity during pyrolysis was reduced, which in turn mitigated the effect of catalyst acidity and surface properties reduction on pyrolysis. Related research has shown that coke is mainly generated from lignin and is positively correlated with the number of strong acid sites (Zheng *et al.* 2014; Zhou *et al.* 2017). Accordingly, the increase of lignin in CS-WT requires the reduction in catalyst acidity, thereby reducing coke formation. The hydrogen-carbon effective ratio (H/Ceff) of CS and CS-WT were -0.19 and 0.17, respectively. This would promote the aromatization reaction of the pyrolysis process and generate more-C-C-bonds and benzene ring structures. The calorific value of CS-WT increased from 17.10 to 20.77 MJ/kg. This means that there was an increase in the energy density of CS-WT, which might increase in the fuel value of bio-oil.

TG analysis

The thermal decomposition behavior curves of CS and CS-WT are shown in Fig. 4. It is shown that the decomposition of CS was accelerated after 163 ℃, while the decomposition rate of CS-WT increased after 228 ℃. After WT, cellulose and lignin were enriched, and the polymerization degree and thermal stability of CS-WT were improved (Zheng *et al.* 2015). The decomposition temperature range of CS was 163 to 362 ℃, and

the weight loss peak was at 321 ℃; while the decomposition temperature range of CS-WT was 228 to 386 ℃, the weight loss peak was at 350 ℃, and CS had a small shoulder at 258 ℃, while CS-WT did not. This result suggests that WT not only can remove hemicellulose, but it also can change part of the structure of lignin and cellulose to make it more thermally stable, such as increasing the crystallite size (Cortés and Bridgwater 2015). The peak weight loss of CS-WT reached 10.85%/min, while that of CS was only 8.70%/min. The enrichment of cellulose and lignin in CS-WT resulted in a more concentrated decomposition interval. Figure 4 shows that the TG curve of CS-WT was always higher than that of CS, and the decomposition continued after 380 ℃, which is because the pyrolysis of lignin is continuous and indistinguishable (He *et al.* 2016).

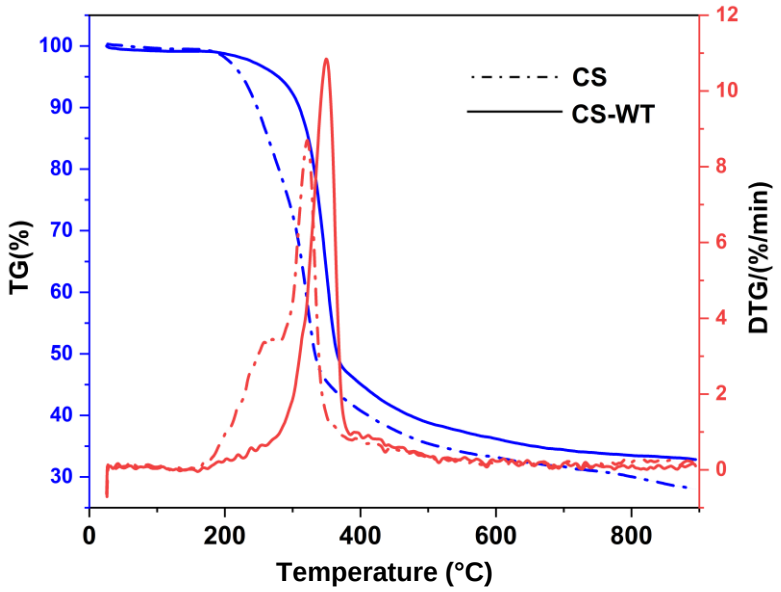

Fig. 4. TG and DTG curves of CS and CS-WT

Mass Fraction of Pyrolysis Products

The yields of products produced by pyrolysis of CS and CS-WT with different catalysts are shown in Fig. 5. After adding the catalyst, the bio-oil and biochar yields of CS and CS-WT were improved, and the mass fraction of non-condensable gas was reduced. The reason for the increase of bio-oil yield is that the catalyst promotes the decomposition reaction of biomass raw materials and generates more condensed gas. The reason for the increase of biochar yield is that excessive catalyst leads to excessive pyrolysis reaction, which causes the polymerization of small molecular products and the formation of macromolecular coke products. During pyrolysis of CS, the yield of biochar increased with the loading of metal on the catalyst, while it changed little during pyrolysis of CS-WT. It is speculated that the acidity of the catalyst has a great influence on the distribution of pyrolysis products during the pyrolysis of CS. However, when the biomass was pretreated by WT, the effect of catalyst acidity on the pyrolysis reaction pathway was weakened due to the removal of hemicellulose. Only Ni-HZSM-5 had higher bio-oil yield during pyrolysis of CS-WT than that of CS. This is because Ni-HZSM-5 has the weakest acidity, which can not only promote biomass pyrolysis to form small molecules, but also minimize the promotion of bio-oil polymerization to form coke.

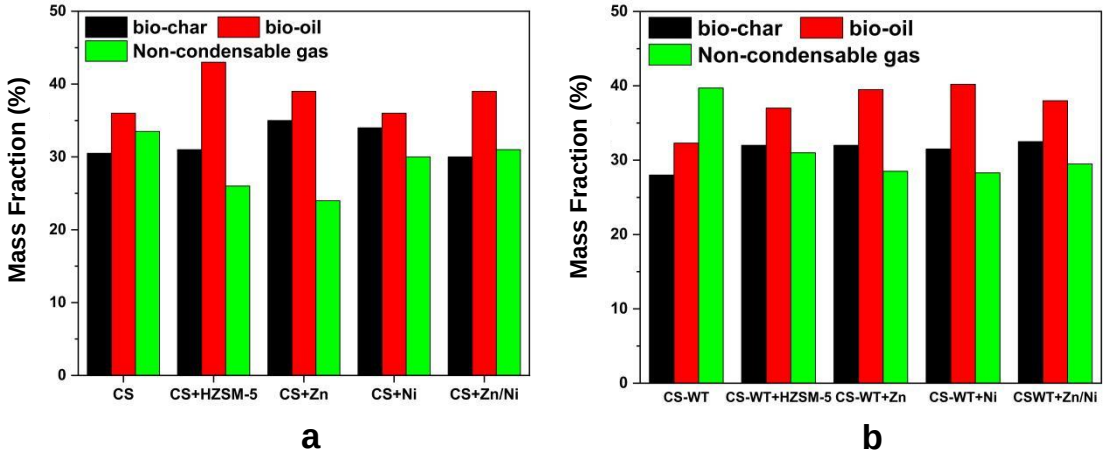

Fig. 5. The mass fraction of pyrolysis products of CS and CS-WT

GC-MS Analysis of Bio-oil

The bio-oil samples were analyzed by GC-MS to study the changes of bio-oil components. Due to the existence of a large number of isomers in the components, they were classified according to differences in functional groups. The main chemical components in bio-oil can be divided into acids, alcohols, esters, ketones, furans, aliphatic hydrocarbons (AHCs), MAHs, PAHs, phenols, and anhydro-sugars.

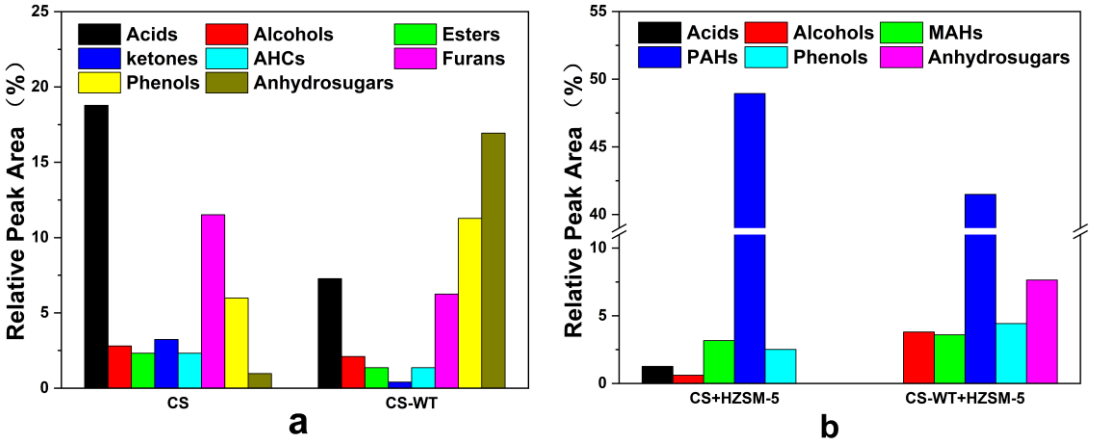

Fig. 6. Comparison of pyrolysis bio-oil of CS and CS-WT

Effects of WT and HZSM-5 on the selectivity of pyrolysis products

The bio-oil components of direct pyrolysis and catalytic pyrolysis with CS and CS-WT are shown in Fig. 6. After WT, the relative content of oxygen functional groups in bio-oil was significantly reduced. The relative peak area of acids decreased from 18.8% to 7.27%, and the furans also decreased from 11.5% to 6.24%. The main acid product was acetic acid, which is mainly produced by the cleavage of acetyl groups in hemicellulose, and furans were derived from the cleavage of glycosidic bonds in cellulose and hemicellulose (Yogalakshmi *et al.* 2022). The decomposition of hemicellulose during WT led to the decrease of acetic acid and furans in the bio-oil (Xu *et al.* 2018). For alcohols and esters, the effect of WT was minimal. The increase of ketones relative content was due to an increase in the cellulose content of the feedstock. Another product that changed greatly was AHCs. In both direct pyrolysis and catalytic pyrolysis of CS, AHCs could be

detected (relative contents were 3.23% and 0.40%, respectively), but could not be detected at all after WT. This indicates that the formation of alkanes is related to the side chain structure of hemicellulose.

After WT, the relative content of anhydro-sugars in bio-oil increased significantly (from 0.97% to 16.93%). There were two reasons: The first is that the cellulose content increased, of which the glycosidic bonds were broken to generate anhydro-sugars (Wu *et al.* 2016). Another reason is that alkali metals and alkaline earth metals were removed, which can catalyze the cleavage of the C-C bond of anhydro-sugars to form small molecular compounds and permanent gases; therefore, the anhydro-sugars generated by pyrolysis were not further decomposed (Shimada *et al.* 2008). The peak area of phenols increased from 5.98% to 11.3% after WT. This is related to the increase of lignin content because phenols are generally generated by the cleavage of ether bonds in lignin (Li *et al.* 2020). In conclusion, in the biomass pyrolysis products after WT, the abundance of oxygenates (especially acids) and furans was greatly reduced, while the abundance of anhydro-sugars increased rapidly. This may mitigate the negative effects of reduced catalyst acidity, make the catalyst more targeted in the selection of loaded metals, and alleviate the carbon deposition.

Unlike direct pyrolysis, almost no oxygenates could be detected in the bio-oil after catalytic pyrolysis of CS and CS-WT, and the components of bio-oil were mainly aromatics and small number of phenols. Compared with direct pyrolysis of CS, the total relative content of oxygenated organics in bio-oil dropped from 48.6% to 1.87% (including acetic acid, propanol ethyl carbinol and butanol) with HZSM-5. The transformation pathways of oxygenates during catalytic pyrolysis were as follows: Firstly, deoxygenations such as decarboxylation, decarbonylation, dehydroxylation, and dehydration occurred on the acidic site of the catalyst to generate oxygen-free short-chain alkanes or alkenes. Then these alkanes and alkenes were diffused into the pores of the catalyst to polymerize and undergo dehydroaromatization or Diels-Alder reactions, and finally generate oxygen-free aromatics (Puertolas *et al.* 2015). In this study, HZSM-5 was able to almost completely convert the oxygenates in the bio-oil of CS to aromatics. It can be speculated that HZSM-5 is sufficient for the aromatization reaction when catalyzing an equivalent amount of CS-WT. This made the reduction in surface properties and acidity acceptable after the catalyst was loaded with metal. HZSM-5 resulted in a decrease in the relative content of anhydro-sugars from 16.9% to 7.64% with CS-WT pyrolysis. The main saccharides produced by cellulose pyrolysis were anhydro-sugars, mainly composed of 1,6-anhydro-β-D-glucopyranose, which are important intermediates for the formation of aromatic compounds in catalytic pyrolysis reactions (Zhang *et al.* 2012). Therefore, after catalytic pyrolysis, anhydro-sugars is largely converted into aromatic products.

Another species whose selectivity decreased with HZSM-5 was phenols. The phenolic relative content of CS and CS-WT decreased from 5.98% and 11.28% to 2.51% and 4.42%, respectively. The phenols in biomass pyrolysis mainly come from the cleavage of ether bonds on the benzene ring structure in lignin. HZSM-5 can promote the decomposition of lignin, but the generated phenols will further undergo dehydroxylation at the acid site. Studies had shown that the phenol generated in the pyrolysis reaction is difficult to convert into aromatic hydrocarbons, which only occurred when there are a large number of strong acid sites (Ma *et al.* 2014). Therefore, in this experiment, the production of phenols after catalytic pyrolysis of HZSM-5 was reduced relative to that of direct pyrolysis. In the above reaction, the main reaction direction of furans and saccharides is deoxyaromatization. Therefore, aromatics were the most important products of CS and CS-

WT pyrolysis with HZSM-5, and their relative contents reached 52.1% and 45.1%, respectively. However, PAHs were the majority, which is higher than reported by Wang *et al.* (2020). There were two reasons for this difference: 1. The ratio of reaction feedstock to catalyst was high, and a large number of strong acid sites led to overreaction, which oligomerized MAHs and converted them into PAHs; 2. The benzene ring generated by pyrolysis stayed in the pores of the catalyst for too long and was not desorbed in time, and therefore the cyclization reaction occurred again with small molecular alkanes or alkenes (Vichaphund *et al.* 2015).

Effects of loaded metal on bio-oils of CS and CS-WT

The main bio-oil components of co-pyrolysis of CS and CS-WT with four catalysts are shown in Fig. 7. The order of the abundance of alcohols was Ni-HZSM-5 > Zn-HZSM-5 > Zn/Ni-HZSM-5 > HZSM-5, but the yields were very small. When the catalyst was loaded, the selectivity decreased the most for phenols. For CS, Zn/Ni-HZSM-5 could completely convert phenols, while the other three catalysts had phenolic relative content between 1.85% and 2.51%. When pyrolyzing CS-WT, the relative content of phenols was 4.42% with HZSM-5, which was much higher than other catalysts. In direct pyrolysis, the phenolic yield of CS was lower than that of CS-WT, indicating that WT created favorable reaction conditions for lignin cracking to generate phenols. However, when using metal-loaded catalyst, the phenolic abundance of CS-WT decreased more greatly, which might be related to the priority of the catalyst deoxygenation reaction. During pyrolysis, the dehydroxylation of phenols has a lower priority than decarboxylation, decarbonylation and other reactions. However, WT reduced the small molecule oxygenates and the acid content of bio-oil, so that the priority of the dephenolic hydroxyl reaction in the pyrolysis process was raised (Ma *et al.* 2014). The loaded metals also promote aromatization of phenols: The metal active sites formed by Ni can promote the dehydrogenation of phenols to form olefins, and it is also possible to directly crack phenols into aromatics (Maia *et al.* 2010). Meanwhile, Zn loading can promote dehydrogenation and aromatization reactions, and convert phenols to hydrocarbons through hydrogenolysis reactions, thereby reducing the phenolic content (Cheng *et al.* 2018). In the pyrolysis reactions of CS and CS-WT, Zn/Ni-HZSM-5 had the best conversion effect on phenols compared to Ni-HZSM-5 and Zn-HZSM-5, which proves the interaction between Zn and Ni.

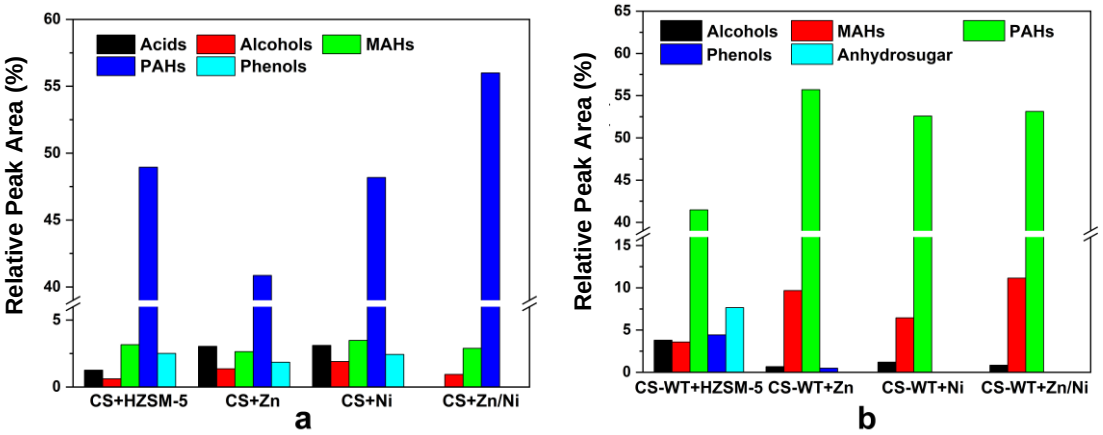

Fig. 7. Liquid-phase product distribution of pyrolysis of CS and CS-WT with four catalysts

The bio-oil of CS-WT with HZSM-5 contained 7.65% anhydro-sugars, but they were not detected with three metal-loaded catalysts. Compared with direct pyrolysis of CS-WT, HZSM-5 promotes the cleavage of anhydro-sugars in bio-oil. Zn and Ni further promote the cleavage of anhydro-sugars into small molecules such as furans, and convert furans into smaller alkene molecules. Polycondensation, aromatization, and cyclization are carried out to generate aromatics (Rezaei *et al.* 2014). In the pyrolysis experiments of CS-WT, HZSM-5 reduced the production of phenols and anhydro-sugars, and completely converted them with metal loading. In the pyrolysis reaction of CS, the optimization of catalysts was not obvious. This indicated that WT optimized the biomass feedstock composition. Therefore, the promoting effect of Zn and Ni on the deoxygenation and aromatization reactions were more obvious. In the bio-oil of catalytic pyrolysis, the most important products are aromatics. The roles of Zn and Ni in the pyrolysis reaction of CS and CS-WT are different, and their selectivities to aromatics are also different. In CS pyrolysis bio-oil, the peak areas of MAHs/ PAHs corresponding to HZSM-5, Zn-HZSM-5, Ni-HZSM-5, Zn/Ni-HZSM-5 were 3.16%/ 48.95%, 2.64%/ 40.86%, 3.48%/ 48.18%, 2.89%/ 56.00%, respectively. By comparison, in CS-WT pyrolysis bio-oil the above data were 3.58%/ 41.48%, 9.67%/ 55.71% , 6.44%/ 52.99%, and 11.14%/ 53.13%, respectively. The catalytic effect of Zn and Ni was obvious in the pyrolysis of CS-WT. Compared with HZSM-5, Zn/ Ni/ Zn/Ni increased the relative content of MAHs by 6.09%/ 2.86%/ 7.56%, respectively; Zn promoted aromatization more than Ni and inhibited the oligomerization of monocyclic aromatic hydrocarbons. However, when the CS was pyrolyzed, Zn and Ni did not improve the abundance of MAHs, but produced more alcohols and acids. This indicates that loaded metal replaced some of the strong acid sites, which reduced the acidity of HZSM-5, resulting in incomplete aromatization of oxygenated compounds (Chen *et al.* 2018). The different roles of loaded metals in CS and CS-WT illustrated that WT pretreatment optimized the composition of biomass and provided conditions for the catalysis of loaded metals. When catalyzing CS, Zn/Ni-HZSM-5 had the highest total aromatic relative content, which might reflect the synergistic effect of Zn and Ni in the catalytic pyrolysis (Xu *et al.* 2010; Cheng *et al.* 2018). This synergy was more evident in the catalytic pyrolysis of CS-WT, which increased the peak area of MAHs to 11.1%.

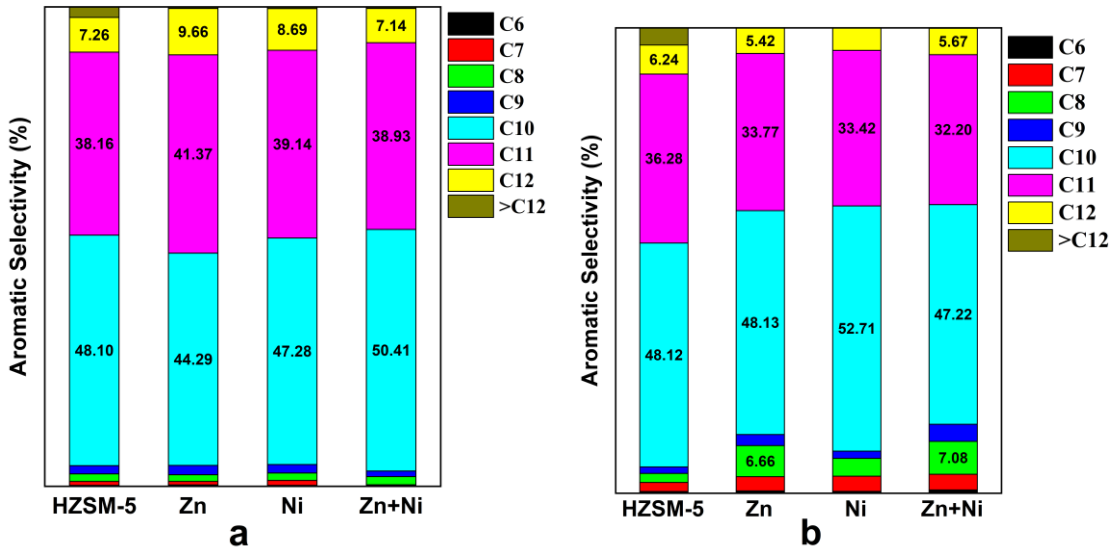

Fig. 8. Aromatic carbon number distribution of pyrolysis products of four catalysts. (a: CS; b: CS-WT)

The aromatics carbon number distribution of bio-oils is shown in Fig. 8. Among the aromatics produced by catalytic pyrolysis of CS, C10, and C11 compounds were the main ones. The relative content of various aromatics changed little, and the catalytic effect of loaded metals was inconspicuous. This was because the CS bio-oil directly pyrolyzed had high acidity and oxygen content.

In the catalytic pyrolysis of CS, the main factor is the acidity of the catalyst, rather than the catalytic properties of the loaded metals (Zhou *et al.* 2017). However, during the catalytic pyrolysis of CS-WT, the selectivity of light aromatics was significantly improved with the metal loading of HZSM-5. Compared with HZSM-5, the yield of C6-C9 after catalytic pyrolysis of Zn-HZSM-5/ Ni-HZSM-5/ Zn/Ni-HZSM-5 increased from 5.66% to 12.60%/ 9.02%/ 14.78%, respectively. This indicated that the optimization of biomass components by WT was conducive to the catalytic effect of the supported metal, thereby improving the selectivity of light aromatics.

It is worth noting that although both Zn and Ni contributed to improving the selectivity of light aromatics, there was significant difference: The selectivity of Zn to C8 and C9 was higher than that of Ni, while the selectivity of Ni to C10 was higher. This is related to the pore distribution of the catalyst: The micropore volume of Ni-HZSM-5 is lower than that of Zn-HZSM-5, but the mesopore volume and pore size are higher, which makes Ni-HZSM-5 have higher selectivity for macromolecular aromatics (Yu *et al.* 2012). Whether in the pyrolysis of CS or CS-WT, the selectivity of Zn/Ni-HZSM-5 to light aromatics was higher than that of Zn-HZSM-5 and Ni-HZSM-5. It presented that the interaction between Zn and Ni during the pyrolysis process is beneficial to the upgrading of pyrolysis bio-oil.

Effects of WT and metal-loaded catalysts on the pyrolysis pathway.

In this study, the direct pyrolysis process of CS has been described previously. After WT, the removal of hemicellulose reduced the yields of acids and furans in the bio-oil, while the enrichment of lignin improved the phenolic relative content. Since the alkali metals and alkaline earth metals were removed, the cellulose was retained after being decomposed into dehydrated sugars without secondary decomposition. Compared with direct pyrolysis, HZSM-5 further optimized the pyrolysis reaction path of CS-WT. Oxygenates (such as acids, ketones and furans) underwent deoxygenation at the acid sites of the catalyst to generate short-chain alkanes or alkenes, which diffused into the pores of the catalyst to undergo dehydroaromatization reaction or Diels-Alder reaction, finally generated aromatics (Puertolas *et al.* 2015).

Another way to generate aromatics is the dehydroxylation of phenols. The enrichment of lignin improved the relative content of phenols, WT raised the priority of the dephenolic hydroxylation reaction (Ma *et al.* 2014). The anhydro-sugars were also catalytically cracked into oxygenates by HZSM-5, which were further converted into aromatics. After loading Zn and Ni, the anhydro-sugars and phenols were completely converted, and the polymerization of MAHs to form PAHs was inhibited. Compared to pyrolysis CS, the supported metals have a stronger degree of optimization for the pyrolysis reaction process of CS-WT. The catalytic effect of Zn/Ni-HZSM-5 in the pyrolysis reaction of CS and CS-WT is higher than that of the two monometallic catalysts, which proved the synergistic effect of Zn and Ni in the catalytic pyrolysis reaction.

CONCLUSIONS

1. Wet torrefaction (WT) removed hemicellulose from corn stalk (CS) and enriched cellulose and lignin. When pyrolyzing feedstocks to produce bio-oil, WT decreased acidity and the selectivity of oxygen-containing small molecules, and phenols and anhydro-sugars became important products.
2. As the yields of other oxygen-containing compounds (especially acids) decreased, dephenolic hydroxylation was easier to react, and the catalytic effect of Zn and Ni was more obvious. Compared with monometallic catalysts, Zn/Ni-HZSM-5 improved the relative selectivity of single-ring aromatics from 9.67% and 6.44% to 11.1%, which is due to the synergistic effect of Zn and Ni in the pyrolysis reaction.
3. With the same catalyst, the total relative contents of aromatics and monocyclic aromatics (MAHs) selectivity of all CS-WT bio-oils were close to or even higher than those of CS bio-oils, indicating that WT provides suitable conditions for the catalyst and loaded metals to play a catalytic role.

ACKNOWLEDGEMENTS

This research was sponsored by the National Natural Science Foundation of China (52130610, 52106258, 52206225), the Distinguished Expert of Taishan Scholars Shandong Province and Youth Science, and Technology Innovation Team of Shandong Colleges and Universities (2021KJ097).

REFERENCES CITED

Bach, Q.-V., Tran, K.-Q., Skreiberg, Ø., and Trinh, T. T. (2015). "Effects of wet torrefaction on pyrolysis of woody biomass fuels," *Energy* 88, 443-456. DOI: 10.1016/j.energy.2015.05.062

Balasundram, V., Ibrahim, N., Kasmani, R. M., Hamid, M. Kamaruddin Abd., Isha, R., Hasbullah, H., and Ali, R. R. (2017). "Catalytic pyrolysis of sugarcane bagasse over cerium (rare earth) loaded HZSM-5 zeolite," *Energy Procedia* 142, 801-808. DOI: 10.1016/j.egypro.2017.12.129

Bjørgen, M., Joensen, F., Spangsberg Holm, M., Olsbye, U., Lillerud, K.-P., and Svelle, S. (2008). "Methanol to gasoline over zeolite H-ZSM-5: Improved catalyst performance by treatment with NaOH," *Applied Catalysis A: General* 345(1), 43-50. DOI: 10.1016/j.apcata.2008.04.020

Chen, H., Cheng, H., Zhou, F., Chen, K., Qiao, K., Lu, X., Ouyang, P., and Fu, J. (2018). "Catalytic fast pyrolysis of rice straw to aromatic compounds over hierarchical HZSM-5 produced by alkali treatment and metal-modification," *Journal of Analytical and Applied Pyrolysis* 131, 76-84. DOI: 10.1016/j.jaap.2018.02.009

Cheng, S., Wei, L., and Rabnawaz, M. (2018). "Catalytic liquefaction of pine sawdust and in-situ hydrogenation of bio-crude over bifunctional Co-Zn/HZSM-5 catalysts," *Fuel* 223, 252-260. DOI: 10.1016/j.fuel.2018.03.043

Cheng, S., Wei, L., Julson, J., Kharel, P. R., Cao, Y., and Gu, Z. (2017). "Catalytic liquefaction of pine sawdust for biofuel development on bifunctional Zn/HZSM-5

catalyst in supercritical ethanol," *Journal of Analytical and Applied Pyrolysis* 126, 257-266. DOI: 10.1016/j.jaap.2017.06.001

Cortés, A. M. and Bridgwater, A. V. (2015). "Kinetic study of the pyrolysis of miscanthus and its acid hydrolysis residue by thermogravimetric analysis," *Fuel Processing Technology* 138, 184-193. DOI: 10.1016/j.fuproc.2015.05.013

Dai, L., Wang, Y., Liu, Y., Ruan, R., Duan, D., Zhao, Y., Yu Z., and Jiang, L. (2019). "Catalytic fast pyrolysis of torrefied corn cob to aromatic hydrocarbons over Ni-modified hierarchical ZSM-5 catalyst," *Bioresource Technology* 272, 407-414. DOI: 10.1016/j.biortech.2018.10.062

Danso, B., and Achaw, O.-W. (2022). "Bioenergy and biofuel production from biomass using thermochemical conversions technologies—A review," *AIMS Energy* 10(4), 585-647. DOI: 10.3934/energy.2022030.

Danso-B., Ross, A. B., Mariner, T., Hammerton, J., and Fitzsimmons, M. (2022). "Hydrochars produced by hydrothermal carbonisation of seaweed, coconut shell and oak: Effect of processing temperature on physicochemical adsorbent characteristics," *SN Applied Sciences* 4(8), DOI: 10.1007/s42452-022-05085-x.

Foster, A. J., Jae, J., Cheng, Y.-T., Huber, G. W., and Lobo, R. F. (2012). "Optimizing the aromatic yield and distribution from catalytic fast pyrolysis of biomass over ZSM-5," *Applied Catalysis A: General* 423-424, 154-161. DOI: 10.1016/j.apcata.2012.02.030

Gao, C., Zhang, J., Xing, E., Xie, Y., Zhao, H., Ning, P., and Shi, Y. (2021). "Upgrading of palmitic acid to diesel-like fuels over Ni@HZSM-5 bi-functional catalysts through the in-situ encapsulation method," *Molecular Catalysis* 511. DOI: 10.1016/j.mcat.2021.111715

Ge, J., Wu, Y., Han, Y., Qin, C., Nie, S., Liu, S., Wang, S., and Yao, S. (2020). "Effect of hydrothermal pretreatment on the demineralization and thermal degradation behavior of eucalyptus," *Bioresource Technology* 307, article 123246. DOI: 10.1016/j.biortech.2020.123246

He, X.-f., Yang, L., Wu, H.-j., Liu, N., Zhang, Y.-g., and Zhou, A.-n. (2016). "Characterization and pyrolysis behaviors of sunflower stalk and its hydrolysis residue," *Asia-Pacific Journal of Chemical Engineering* 11(5), 803-811. DOI: 10.1002/apj.2015

Huang, M., Ma, Z., Zhou, B., Yang, Y., and Chen, D. (2020). "Enhancement of the production of bio-aromatics from renewable lignin by combined approach of torrefaction deoxygenation pretreatment and shape selective catalytic fast pyrolysis using metal modified zeolites," *Bioresource Technology* 301, article 122754. DOI: 10.1016/j.biortech.2020.122754

Li, J., Zhao, P., Li, T., Lei, M., Yan, W., and Ge, S. (2020). "Pyrolysis behavior of hydrochar from hydrothermal carbonization of pinewood sawdust," *Journal of Analytical and Applied Pyrolysis* 146, 10. DOI: 1016/j.jaap.2020.104771.

Li, Z., Zhong, Z., Zhang, B., Wang, W., Seufitelli, G. V. S., and Resende, F. L. P. (2020). "Catalytic fast co-pyrolysis of waste greenhouse plastic films and rice husk using hierarchical micro-mesoporous composite molecular sieve," *Waste Manag* 102, 561-568. DOI: 10.1016/j.wasman.2019.11.012

Liang, J., Morgan, H. M., Liu, Y., Shi, A., Lei, H., Mao H., and Bu, Q. (2017). "Enhancement of bio-oil yield and selectivity and kinetic study of catalytic pyrolysis of rice straw over transition metal modified ZSM-5 catalyst," *Journal of Analytical and Applied Pyrolysis* 128, 324-334. DOI: 10.1016/j.jaap.2017.09.018

Liu, D., Cao, L., Zhang, G., Zhao, L., Gao, J., and Xu, C. (2021). "Catalytic conversion

of light alkanes to aromatics by metal-containing HZSM-5 zeolite catalysts—A review," *Fuel Processing Technology* 216. DOI: 10.1016/j.fuproc.2021.106770

Liu, Q., Wang, J., Zhou, J., Yu, Z., and Wang, K. (2021). "Promotion of monocyclic aromatics by catalytic fast pyrolysis of biomass with modified HZSM-5," *Journal of Analytical and Applied Pyrolysis* 153. DOI: 10.1016/j.jaap.2020.104964

Lu, Q., Li, W.-Z., and Zhu, X.-F. (2009). "Overview of fuel properties of biomass fast pyrolysis oils," *Energy Conversion and Management* 50(5), 1376-1383. DOI: 10.1016/j.enconman.2009.01.001

Ma, Z., Custodis, V., and van Bokhoven, J. A. (2014). "Selective deoxygenation of lignin during catalytic fast pyrolysis," *Catalysis Science & Technology* 4(3). DOI: 10.1039/c3cy00704a

Maia, A. J., Louis, B., Lam, Y. L., and Pereira, M. M. (2010). "Ni-ZSM-5 catalysts: Detailed characterization of metal sites for proper catalyst design," *Journal of Catalysis* 269(1), 103-109. DOI: 10.1016/j.jcat.2009.10.021

Puertolas, B., Veses, A., Callen, M. S., Mitchell, S., Garcia, T., and Perez-Ramirez, J. (2015). "Porosity-acidity interplay in hierarchical ZSM-5 zeolites for pyrolysis oil valorization to aromatics," *ChemSusChem* 8(19), 3283-3293. DOI: 10.1002/cssc.201500685.

Qiao, K., Zhou, F., Han, Z., Fu, J., Ma, H., and Wu, G. (2019). "Synthesis and physicochemical characterization of hierarchical ZSM-5: Effect of organosilanes on the catalyst properties and performance in the catalytic fast pyrolysis of biomass," *Microporous and Mesoporous Materials* 274, 190-197. DOI: 10.1016/j.micromeso.2018.07.028

Rezaei, P. S., Shafaghat, H., and Daud, W. M. A. W. (2014). "Production of green aromatics and olefins by catalytic cracking of oxygenate compounds derived from biomass pyrolysis: A review," *Applied Catalysis A: General* 469, 490-511. DOI: 10.1016/j.apcata.2013.09.036

Rostamizadeh, M., Yaripour, F., and Hazrati, H. (2018). "Ni-doped high silica HZSM-5 zeolite (Si/Al = 200) nanocatalyst for the selective production of olefins from methanol," *Journal of Analytical and Applied Pyrolysis* 132, 1-10. DOI: 10.1016/j.jaap.2018.04.003

Shimada, N., Kawamoto, H., and Saka, S. (2008). "Different action of alkali/alkaline earth metal chlorides on cellulose pyrolysis," *Journal of Analytical and Applied Pyrolysis* 81(1), 80-87. DOI: 10.1016/j.jaap.2007.09.005

Tursunov, O., Kustov, L., and Tilyabaev, Z. (2019). "Catalytic activity of H-ZSM-5 and Cu-HZSM-5 zeolites of medium SiO2/Al2O3 ratio in conversion of n-hexane to aromatics," *Journal of Petroleum Science and Engineering* 180, 773-778. DOI: 10.1016/j.petrol.2019.06.013

Yogalakshmi, K. N., Poornima Devi, T., Sivashanmugan, P., Kavitha, S., Kannah, R. Y., Varjani, S., AdhishKumar, S., Kumar, G., and Banu J., R. (2022). "Lignocellulosic biomass-based pyrolysis: A comprehensive review," *Chemosphere* 286 (Pt 2), article 131824. DOI: 10.1016/j.chemosphere.2021.131824

Vichaphund, S., Aht-ong, D., Sricharoenchaikul, V., and Atong, D. (2015). "Production of aromatic compounds from catalytic fast pyrolysis of Jatropha residues using metal/HZSM-5 prepared by ion-exchange and impregnation methods," *Renewable Energy* 79, 28-37. DOI: 10.1016/j.renene.2014.10.013

Vitale, G., Molero, H., Hernandez, E., Aquino, S., Birss, V., and Pereira-Almao, P. (2013). "One-pot preparation and characterization of bifunctional Ni-containing

ZSM-5 catalysts," *Applied Catalysis A: General* 452, 75-87. DOI: 10.1016/j.apcata.2012.11.026

Wang, S., Dai, G., Yang, H., and Luo, Z. (2017). "Lignocellulosic biomass pyrolysis mechanism: A state-of-the-art review," *Progress in Energy and Combustion Science* 62, 33-86. DOI: 10.1016/j.pecs.2017.05.004

Wang, X., Wu, J., Chen, Y., Pattiya, A., Yang, H., and Chen, H. (2018). "Comparative study of wet and dry torrefaction of corn stalk and the effect on biomass pyrolysis polygeneration," *Bioresource Technology* 258, 88-97. DOI: 10.1016/j.biortech.2018.02.114

Wang, Y., Ke, L., Peng, Y., Yang, Q., Liu, Y., Wu, Q., Tang, Y., Zhu, H., Dai, L., Zeng, Z., Jiang, L., and Ruan, R. (2020). "*Ex-situ* catalytic fast pyrolysis of soapstock for aromatic oil over microwave-driven HZSM-5@SiC ceramic foam," *Chemical Engineering Journal* 402. DOI: 10.1016/j.cej.2020.126239

Wu, S., Shen, D., Hu, J., Zhang, H., and Xiao, R. (2016). "Cellulose-lignin interactions during fast pyrolysis with different temperatures and mixing methods," *Biomass and Bioenergy* 90, 209-217. DOI: 10.1016/j.biombioe.2016.04.012

Xu, J., Liao, Y., Lin, Y., Ma, X., and Yu, Z. (2019). "Study on catalytic pyrolysis of eucalyptus to produce aromatic hydrocarbons by Zn-Fe co-modified HZSM-5 catalysts," *Journal of Analytical and Applied Pyrolysis* 139, 96-103. DOI: 10.1016/j.jaap.2019.01.014

Xu, J., Zhang, S., Shi, Y., Zhang, P., Huang, D., Lin, C., and Wu, Y. (2022). "Upgrading the wood vinegar prepared from the pyrolysis of biomass wastes by hydrothermal pretreatment," *Energy* 244. DOI: 10.1016/j.energy.2021.122631

Xu, X., Tu, R., Sun, Y., Li, Z., and Jiang, E. (2018). "Influence of biomass pretreatment on upgrading of bio-oil: Comparison of dry and hydrothermal torrefaction," *Bioresource Technology* 262, 261-270. DOI: 10.1016/j.biortech.2018.04.037

Xu, Y., Wang, T., Ma, L., Zhang, Q., and Liang, W. (2010). "Upgrading of the liquid fuel from fast pyrolysis of biomass over MoNi/γ-Al2O3 catalysts," *Applied Energy* 87 (9), 2886-2891. DOI: 10.1016/j.apenergy.2009.10.028

Yu, Y., Li, X., Su, L., Zhang, Y., Wang, Y., and Zhang, H. (2012). "The role of shape selectivity in catalytic fast pyrolysis of lignin with zeolite catalysts," *Applied Catalysis A: General* 447-448, 115-123. DOI: 10.1016/j.apcata.2012.09.012

Zhang, D., Wang, F., Shen, X., Yi, W., Li, Z., Li, Y., and Tian, C. (2018). "Comparison study on fuel properties of hydrochars produced from corn stalk and corn stalk digestate," *Energy* 165, 527-536. DOI: 10.1016/j.energy.2018.09.174

Zhang, X., Yang, W., and Blasiak, W. (2012). "Thermal decomposition mechanism of levoglucosan during cellulose pyrolysis," *Journal of Analytical and Applied Pyrolysis* 96, 110-119. DOI: 10.1016/j.jaap.2012.03.012

Zhao, X., Wei, L., Julson, J., Gu, Z., and Cao, Y. (2015). "Catalytic cracking of inedible camelina oils to hydrocarbon fuels over bifunctional Zn/ZSM-5 catalysts," *Korean Journal of Chemical Engineering* 32(8), 1528-1541. DOI:10.1007/s11814-015-0028-8

Zheng, A., Zhao, Z., Chang, S., Huang, Z., Wu, H., Wang, X., He, F., and Li, H. (2014). "Effect of crystal size of ZSM-5 on the aromatic yield and selectivity from catalytic fast pyrolysis of biomass," *Journal of Molecular Catalysis A: Chemical* 383-384, 23-30. DOI: 10.1016/j.molcata.2013.11.005

Zheng, A., Zhao, Z., Chang, S., Huang, Z., Zhao, K., Wei, G., He, F., and Li, H. (2015). "Comparison of the effect of wet and dry torrefaction on chemical structure and pyrolysis behavior of corncobs," *Bioresource Technology* 176, 15-22. DOI: 10.1016/j.biortech.2014.10.157

Zheng, Y., Wang, F., Yang, X., Huang, Y., Liu, C., Zheng, Z., and Gu, J. (2017). "Study on aromatics production via the catalytic pyrolysis vapor upgrading of biomass using metal-loaded modified H-ZSM-5," *Journal of Analytical and Applied Pyrolysis* 126, 169-179. DOI: 10.1016/j.jaap.2017.06.011

Zhou, F., Gao, Y., Ma, H., Wu, G., and Liu, C. (2017a). "Catalytic aromatization of methanol over post-treated ZSM-5 zeolites in the terms of pore structure and acid sites properties," *Molecular Catalysis* 438, 37-46. DOI: 10.1016/j.mcat.2017.05.018

Zhou, F., Gao, Y., Wu, G., Ma, F., and Liu, C. (2017b). "Improved catalytic performance and decreased coke formation in post-treated ZSM-5 zeolites for methanol aromatization," *Microporous and Mesoporous Materials* 240, 96-107. DOI: 10.1016/j.micromeso.2016.11.014

Article submitted: April 7, 2023; Peer review completed: May 7, 2023; Revised version received and accepted: May 21, 2023; Published: May 25, 2023.
DOI: 10.15376/biores.18.3.4897-4915